# Relaxation of NH($a^1\Delta$, $v = 1$) in Collisions with H($^2$S): An Experimental and Theoretical Study[†]

**P. Defazio,[‡] C. Petrongolo,*[,‡,§] G. C. McBane,[||] L. Adam,[⊥] W. Hack,[⊥] S. Akpinar,[#] and R. Schinke[▽]**

*Dipartimento di Chimica, Università di Siena, Via A. Moro 2, I-53100 Siena, Italy, Istituto per i Processi Chimico-Fisici del CNR, Via G. Moruzzi 1, I-56100 Pisa, Italy, Department of Chemistry, Grand Valley State University, Allendale, Michigan 49401, Max-Planck-Institut für Biophysikalische Chemie, D-37077 Göttingen, Germany, Department of Physics, Firat University, 23169 Elazig, Turkey, and Max-Planck-Institut für Dynamik und Selbstorganisation, D-37073 Göttingen, Germany*

*Received: April 27, 2009; Revised Manuscript Received: June 3, 2009*

Collisions of electronically and vibrationally excited NH($a^1\Delta$, $v = 1$) with H atoms were investigated by experimental, quantum mechanical (QM) wavepacket, and quasiclassical trajectory (QCT) methods. The NH($a^1\Delta$, $v = 1$) total loss rate constant, corresponding to the sum of the NH vibrational relaxation, N($^2D$)+$H_2$ formation, and electronic quenching to NH($X^3\Sigma^-$), was measured at room temperature. Most of the calculations were performed within the Born−Oppenheimer approximation, neglecting electronic quenching due to Renner−Teller coupling because QCT calculations showed that for the loss of NH($a^1\Delta$, $v = 1$) the contribution of quenching is negligible. The QM study included Coriolis couplings, and the QCT study counted only trajectories ending close to a vibrational quantum level of the product diatom. The collisions are dominated by long-lived intermediate complexes, and QM probabilities and cross sections thus exhibit pronounced resonances. QM and QCT cross sections and rate coefficients of the various processes are in very good agreement. The measured rate constant is $(9.1 \pm 3.3) \times 10^{-11}$ cm$^3$ s$^{-1}$, compared with $(14.4 \pm 0.5) \times 10^{-11}$ and $(15.6 \pm 1.6) \times 10^{-11}$ cm$^3$ s$^{-1}$, as obtained from QM and QCT calculations, respectively. The reason for the theoretical overestimation is unknown.

## 1. Introduction

The $NH_2$ molecule offers plenty of opportunities for studying molecular dynamics experimentally and theoretically. Spectroscopy of $NH_2(\tilde{X})$ and $NH_2(\tilde{A})$,[1−3] reactions of N($^4S$)[4,5] and N($^2D$) with $H_2$,[6] and reactions of NH($X^3\Sigma^-$)[7,8] and NH($a^1\Delta$)[9] with H are all experimentally accessible. The number of electrons is small enough to permit the calculation of accurate global potential energy surfaces (PESs), and the intra- and intermolecular dynamics can be studied by exact methods. The PESs for the two lowest $NH_2$ doublet states $\tilde{X}^2A''$ and $\tilde{A}^2A'$, which connect the N($^2D$) + $H_2$, NH($X^3\Sigma^-$) + H, and NH($a^1\Delta$) + H asymptotic channels, are particularly important. Both PESs have been computed by several different groups.[8,10−13] The potentials have deep attractive wells, so bimolecular reactions occurring on them are dominated by long-lived complexes.

The reaction N($^2D$) + $H_2$ → NH($X^3\Sigma^-$) + H is exothermic and has been intensively studied.[14] The reaction of NH with H atoms, on the other hand, has received much less attention.[7−9] The reaction of electronically excited NH($a^1\Delta$) with H (or isotopic variants of it) is particularly intriguing because in addition to isotope exchange and the formation of $H_2$, it offers the possibility of electronic quenching of NH. The latter process involves a nonadiabatic $\tilde{A} \rightarrow \tilde{X}$ transition induced by Renner−Teller (RT) coupling near linear H−N−H geometries. In a recent experiment, Adam et al.[9] measured the room-temperature rate coefficient for loss of NX($a^1\Delta$, $v = 0$) in collisions with Y, where X and Y stand for H or D. Here loss involves the exchange reaction if X ≠ Y, the formation of XY, and the production of NX($X^3\Sigma^-$) and NY($X^3\Sigma^-$). In addition, the rate coefficients for the pure quenching processes were determined. The experiments were accompanied by trajectory surface hopping (TSH) calculations including RT coupling.[9] The coupling was described with a single empirical parameter that was adjusted to reproduce the quenching rate for one of the isotope combinations and then also used for the others. With this adjustment, satisfactory agreement with the majority of experimental data was achieved. Akpinar et al.[15] subsequently studied the reaction of NH($a^1\Delta$, $v = 0$) with H by a quantum mechanical (QM) wavepacket (WP) method that ignored the RT coupling. The QM rate coefficient for loss of NH($a^1\Delta$, $v = 0$) agreed well with the experimental and TSH data after subtraction of the rate coefficient for quenching.

In the present work, we extend the previous investigations and consider the collision of electronically and vibrationally excited NH($a^1\Delta$, $v = 1$) with H, which adds the possibility of vibrational relaxation. In particular, we study the following seven processes

[†] Part of the "Vincenzo Aquilanti Festschrift".

* To whom correspondence should be addressed. E-mail: petrongolo@unisi.it.
[‡] Università di Siena.
[§] Istituto per i Processi Chimico-Fisici del CNR.
[||] Grand Valley State University.
[⊥] Max-Planck-Institut für Biophysikalische Chemie.
[#] Firat University.
[▽] Max-Planck-Institut für Dynamik und Selbstorganisation.

10.1021/jp903839p 
Published on Web 07/01/2009

$$NH(a,1) + H' \rightarrow NH(a,1) + H' \quad (1a)$$

$$\rightarrow NH(a,0) + H' \quad (1b)$$

$$\rightarrow NH'(a,1) + H \quad (1c)$$

$$\rightarrow NH'(a,0) + H \quad (1d)$$

$$\rightarrow N(^2D) + H_2 \quad (1e)$$

$$\rightarrow NH(X) + H' \quad (1f)$$

$$\rightarrow NH'(X) + H \quad (1g)$$

where $a$ labels the NH excited $a^1\Delta$ electronic species, $X$ labels the ground $X^3\Sigma^-$ species, and 1 and 0 indicate the vibrational quantum number. Equations 1a and 1b describe vibrationally elastic and inelastic collisions without H-atom exchange, whereas eqs 1c and 1d represent elastic and inelastic collisions with accompanying exchange. Equation 1e is NH depletion into the N($^2D$) + $H_2$ channel, and eqs 1f and 1g stand for the electronic quenching of NH($a$) without and with H-atom exchange.

In this article, we report experimental measurements of the rate coefficient for loss of NH($a$,1). Processes 1b and 1d−1g contribute to the observed loss rate, and the measured second-order rate coefficient is simply the sum of the elementary coefficients for those processes. We present QM calculations for reactions 1b, 1d, and 1e, which are here simply called inelastic, exchange, and depletion, respectively. In the quantum calculations, we use the Born−Oppenheimer (BO) approximation on the $\tilde{A}^2A'$ excited PES without RT coupling to the electronic ground state. Electronic quenching is thus not considered. We also report two types of quasiclassical trajectory (QCT) calculations. One set uses the BO approximation for comparison with QM data, and the other set includes RT coupling with the TSH method for estimating the contribution of the electronic quenching reactions 1f and 1g.

## 2. Experimental Procedures and Results

The experimental setup has been described elsewhere,[16] and only the essentials are repeated here. The experiments were performed at room temperature (298 K) in a quasistatic laser flash photolysis/laser-induced fluorescence (LIF) system; the flow through the reaction cell was negligible between the pump and the probe pulses but sufficient to exchange the gas volume in the 100 ms between pump pulses and to transport the H atoms. The carrier gas was He at a total pressure of 7 mbar. The NH($a$) was produced by photolysis of $HN_3$ at 248 nm. The NH($a$) vibrational populations after photolysis were 32.8, 46.8, 6.9, 3.8, and 0.2% in $v = 0$ to 4, respectively.[17] NH($a$,1) was detected by undispersed fluorescence after dye laser excitation of the $P(2)$ line of the NH($c^1\Pi$,1 ← $a^1\Delta$,1) transition at $\lambda =$ 337.46 nm. NH($a$,0) was detected as described by Adam et al.[9]

The H atoms were generated in a side arm of the reactor in a microwave discharge of an $H_2$/He mixture (5% mole fraction $H_2$ in He). During the experiments, concentration profiles for NH($a$,0) and NH($a$,1) were measured under otherwise identical conditions, and the H atom concentration determined from the known rate coefficients for the reaction NH($a$,0) + H → products.[17] The initial H atom concentration was verified with a titration with $NO_2$ via the reaction H + $NO_2$ → OH + NO. In the titration experiment, the increase in OH with increasing $NO_2$ was observed by LIF.[9]

**TABLE 1: Data from Six Independent Experiments[a]**

| $p$[b] | $[H_2]$[c] | [H][c] | $k_+$[d] | $k_-$[d] | $k_{first}$[d] | $k_{loss}$[e] |
|---|---|---|---|---|---|---|
| 7.1 | 1.3 | 0.67 | 2.56 | 2.22 | 0.34 | 8.4 |
| 6.9 | 1.3 | 0.9 | 2.20 | 1.67 | 0.53 | 9.8 |
| 6.9 | 2.6 | 1.3 | 3.12 | 2.41 | 0.71 | 9.1 |
| 7.0 | 2.6 | 0.97 | 2.82 | 2.25 | 0.57 | 9.8 |
| 7.0 | 5.2 | 1.5 | 3.05 | 2.23 | 0.82 | 9.1 |
| 7.0 | 5.2 | 1.5 | 2.82 | 2.09 | 0.73 | 8.1 |

[a] In all cases, $[HN_3] = 3.4 \times 10^{-11}$ mol cm$^{-3}$, and the data were collected over the time interval $0 \le t_R \le 220$ $\mu$s. $k_{first}$ is the effective first-order rate coefficient for loss of NH($a$,1) by reaction with H. [b] Millibar. [c] $10^{-11}$ mol cm$^{-3}$. [d] 1000/s. [e] $10^{-11}$ cm$^3$ s$^{-1}$.

Gases with the highest commercially available purity were used: He, 99.999%, Praxair; Xe, 99.998%, Messer-Griesheim; $N_2$, 99.995%, UCAR; $NO_2$, 99.5%, Merck; $H_2$, 99.999%, Praxair. We synthesized $HN_3$ by melting stearic acid (97.0%, Merck) with $NaN_3$ (99.0%, Merck).

The loss of NH($a$,1) in collisions with H atoms was measured under pseudo-first-order conditions, that is, $[NH(a,1)]_0 \ll [H(^2S)]_0$, with the reaction time, $t_R$, in the range of 0−220 $\mu$s. The experimental details are given in Table 1. The difference between the rate constants $k_+$ with H atoms present and $k_-$ without H atoms (discharge "on" and "off") yields the effective first-order rate constant, $k_{first}$, for the loss of NH($a$,1). Division by [H] then yields the second-order loss rate coefficient $k_{loss}$.

The loss of NH($a$) in the absence of H atoms is mainly due to the reaction with $HN_3$. The reaction of NH($a$) with $H_2$ at the given $H_2$ concentration contributes about 10% of the first-order rate in the absence of H, assuming that NH($a$,0) and NH($a$,1) react with $H_2$ with similar rate coefficients. The effect of the change in $[H_2]$ due to the discharge can be neglected.[18]

The measurements were performed at a pressure of about 7 mbar. The H atom concentration was varied in the range of (0.67 to 1.5) $\times 10^{-11}$ mol/cm$^3$. It was not possible to vary [H] over a wider range; therefore, the variation of the first-order rate constant with [H] could not be investigated. The final rate coefficient of $(9.1 \pm 3.3) \times 10^{-11}$ cm$^3$ s$^{-1}$ represents the average of six different measurements. The large uncertainty mainly reflects the uncertainty in [H], which is determined from the rate of the reaction NH($a$,0) + H → products and the loss of precision caused by the large background rate in the absence of H atoms.

## 3. Quantum Mechanical Calculations

Because NH is in a $^1\Delta$ electronic state, the associated rotational levels exist[15] for $j \ge 2$. In this work, we consider $j =$ 2, 3, 4, and 5, collision energies $E_{col} \le 0.4$ eV, and temperatures $T \le 500$ K.

We calculated BO coupled-channel (CC) initial-state-resolved probabilities $P_{jK}^{Jp}(E_{col})$ with the real WP method,[19,20] propagating WPs in reactant $R$, $r$, and $\gamma$ or in product $R'$, $r'$, and $\gamma'$ Jacobi coordinates. Here $J$ is the total angular momentum, $p = \pm$ is the total parity, and $K$ is the projection of both $J$ and $j$ on the initial $R$. Inelastic and depletion probabilities were obtained via reactant propagation and asymptotic or flux analysis at $R_\infty = 8$ or $r_\infty = 9$ $a_0$, respectively. Product propagation and asymptotic analysis at $R'_\infty = 8$ $a_0$ gave exchange probabilities. We considered Coriolis couplings between all $J$ projections $\Omega$ on $R$ or $R'$. Other numerical details were reported in ref[15] In particular, we performed $j = 2$ CC calculations at all $J \le 33$; $j = 3$ and 4 CC calculations at all $J \le 15$ and at $J = 20$, 25,

and 30; and finally $j = 5$ CC calculations at all $J \leq 7$ and also at $J = 10$, 15, 20, 25, and 30. These are in total 317 WP propagations. Because these calculations are very expensive, partial wave probabilities were then interpolated for other $J$, as described in ref 15. This approach gave converged cross sections $\sigma_j(E_{col})$ up to 0.4 eV and rate constants $k_j(T)$ up to 500 K.

## 4. Quasiclassical Calculations

We performed two sets of QCT calculations. The first used only the upper $\tilde{A}^2A'$ surface and employed a special trajectory rejection procedure to account for the effects of zero-point energy (ZPE) on the cross sections. The second used both $\tilde{X}^2A''$ and $\tilde{A}^2A'$ PESs and the empirical RT coupling procedure described earlier[9] to provide an estimate of the importance of nonadiabatic transitions to the loss rate.

The classical model does not include the electronic angular momentum of the $a^1\Delta$ state. In all comparisons between quantum and quasiclassical results, we compare results corresponding to the same value of the nuclear rotational quantum number, $N$, rather than the total angular momentum quantum number, $j$. That is, we compare quasiclassical $j_{cl} = 0$ with quantum $j = 2$, and so on. We label results involving both types of calculations with the $j$ value appropriate to the quantum calculations.

**4.1. Single-State Calculations.** We performed QCT calculations starting in $v = 1$ of the NH $a^1\Delta$ state. We used a suitably modified version of the CLASTR program of Muckerman.[21] Most details of the calculations were as described by Adam et al.,[9] but the nonadiabatic coupling mechanism they used was turned off. Trajectories therefore remained on the $NH_2$ $\tilde{A}^2A'$ surface.

The zero-point energies in NH($a$) + H and N($^2D$) + $H_2$ channels can play an important role in the dynamics. In the quasiclassical calculations, the NH($a$) reactant begins with vibrational energy corresponding to the $v = 1$ quantum level. However, during the trajectory, the total vibrational energy is not constrained, and at termination, most trajectories have vibrational energies that do not correspond to quantum levels of the diatomic product. When the ZPE is comparable to the kinetic energy in the exit channel, as is the case here for both NH($a$) + H and N($^2D$) + $H_2$ channels, the classical approximation can introduce substantial errors in product branching ratios.

To address this problem we have used a special trajectory analysis method similar to those described by Varandas et al.[22] and Fleurat-Lessard et al.[23] The basic approach is to exclude from analysis all trajectories that do not terminate with vibrational energies close to some quantum level of the diatomic product. A simple implementation of this idea does not work because most trajectories that remove NH($a$,1) do not meet the selection criterion, whereas trajectories with large impact parameters $b$ that represent "misses" do meet the criterion. Cross sections computed with the usual formula $\sigma_i = \pi b_{max}^2(N_i/N_{tot})$ therefore do not converge with increasing $b_{max}$. Because, essentially, all loss of NH($a$,1) goes through long-lived complexes, a better approach is available.

For each trajectory, we determined a "minimum exchange" count, $M$, as described by Adam et al.[9] We count one minimum exchange each time the shortest atom−atom distance in the system switches from one pair of atoms to another. A glancing collision, for example, will have $M = 0$, and a direct A + BC → AB + C reaction will have $M = 1$. We define a complex-forming trajectory as one with $M \geq 2$. From each set of trajectories with specified initial $v$, $j$, and collision energy, we determined a complex formation cross section $\sigma_{CF} = \pi b_{max}^2(N_{CF,tot}/N_{tot})$, where $N_{CF,tot}$ is the total number of complex-forming trajectories (without regard to the ZPE criterion) and $N_{tot}$ is the total number of trajectories in the run. It is reasonable to ignore the ZPE criterion in determination of $\sigma_{CF}$ because the complex formation stage occurs on the long-range and deeply attractive parts of the potential, and ZPE effects should be negligible.

**TABLE 2: QCT Cross Sections in square angstroms for Removal Processes at $E_{col} = 0.026$ eV, with Initial $j_{cl} = 2$, Computed from the Same Set of Trajectories with Normal and "Picky" Counting**

| | $v = 1$ | | $v = 0$ | |
|---|---|---|---|---|
| | normal | picky | normal | picky |
| NH($v = 0$) + H′ | 9.2 | 10.6 | | |
| NH′($v = 0$) + H | 2.6 | 2.5 | 2.8 | 2.3 |
| NH′($v = 1$) + H | 0.9 | 0.5 | | |
| N($^2D$) + $H_2$($v = 0$) | 1.6 | 1.4 | 3.3 | 5.0 |
| N($^2D$) + $H_2$($v = 1$) | 0.3 | 0.3 | | |

We then discarded all trajectories for which the final vibrational energy, $E_{vib}$, differed from an allowed vibrational level of the diatomic product [either NH($a$) or $H_2$] by more than 5% of the vibrational spacing for that product. Then, we computed cross sections into each channel according to $\sigma_i = \sigma_{CF}N_i/N_{CF}$, where $N_{CF}$ is the number of complex-forming trajectories that met the selection criterion. We checked that the number of trajectories that removed NH($a$,1) with $M < 2$ was negligible and that the distribution of total angular momenta, $J$, in the selected trajectories was not substantially different from that of all complex-forming trajectories.

This "picky counting" procedure gave results that converged appropriately with the width of the selection bin and with the maximum impact parameter, $b_{max}$. Its disadvantage, of course, is cost: of 93 000 total trajectories computed for $v = 1$, $j_{cl} = 2$, and $E_{col} = 0.026$ eV, only 2524 gave complex-forming trajectories that met the ZPE selection criterion. For a specified statistical uncertainty in the results, the cost is therefore about 35 times higher than normal trajectory analysis.

Table 2 shows results for single-state QCT calculations for initial $j_{cl} = 2$, $E_{col} = 0.026$ eV, and both $v = 1$ and $v = 0$ using normal and picky counting to illustrate the effects of the different analysis procedures. The main effect of the picky counting procedure is to reduce the cross sections into the highest product channels. For initial $v = 1$, picky counting has a minor effect; it increases the cross section for pure relaxation and reduces the cross section for exchange into $v = 1$. For initial $v = 0$, the effects are more substantial; picky counting reduces the importance of exchange, which is energetically neutral if ZPE effects are included, and substantially increases the importance of the exothermic N($^2D$) + $H_2$ product channel.

**4.2. Two-State Calculations.** To estimate the overall contribution of nonadiabatic transitions to the $v = 1$ loss rate, we also carried out QCT calculations using the empirical RT model described by Adam et al.[9] In that model, a single parameter, $P$, describes the probability of an RT transition from the $A'$ to the $A''$ state each time the vibrating complex passes near linearity. Adam et al.[9] chose the value $P = 0.0051$ to make the model fit the observed total quenching rate for the NH + H isotope combination. If the complex formation rate predicted by the QCT calculations on the upper surface is accurate, then this model should give a reasonable estimate of the importance of RT transitions for the vibrational relaxation process. During these calculations we used "normal" rather than "picky" trajectory counting; that is, no accounting was made for ZPE effects.

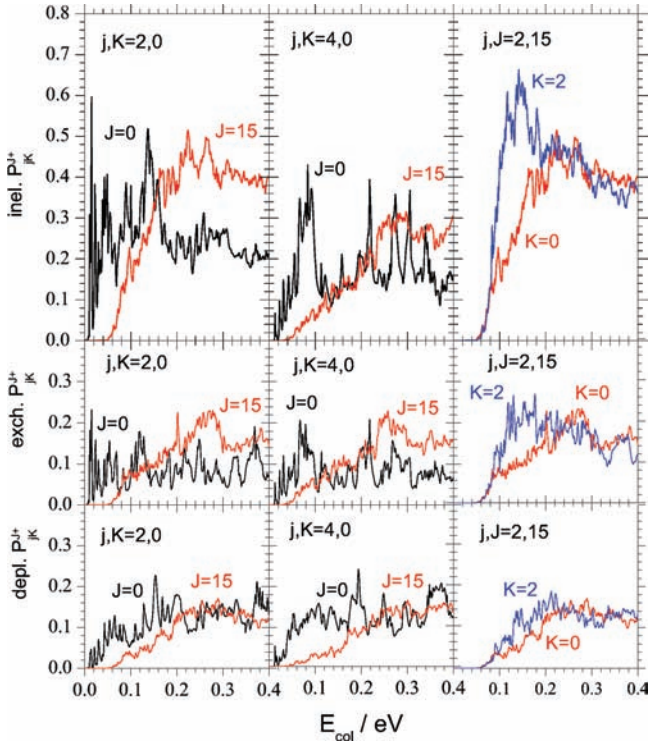


**Figure 1.** BO QM reaction probabilities $P^{J+}_{jK}$ for inelastic to NH($a$,0) + H′, exchange to NH′($a$,0) + H, and depletion to N($^2D$) + $H_2$.

At 300 K, the model including RT effects gives a total $v = 1$ loss rate of $15.4 \times 10^{-11}$ cm$^3$ s$^{-1}$. Processes involving RT transitions contribute merely $0.66 \times 10^{-11}$ of that total. When the empirical RT coupling is turned off, the predicted loss rate is $15.3 \times 10^{-11}$cm$^3$ s$^{-1}$, barely changed from the nonadiabatic model.

The complex formation rate is unaffected by the possibility of RT transitions. Complex formation events that result in RT transitions when those are available find other exit channels when the RT coupling is turned off, and most of those new channels still contribute to loss of NH($a$,1). Simple analysis of the trajectories shows that about 77% of complex formation events produce products other than NH($a$,1), so it is not surprising that the small contribution of RT transitions to the loss rate is made up by other loss mechanisms when the RT coupling is turned off. We conclude that a single-surface, BO model of the total loss rate should be adequate.

## 5. Reaction Probabilities

Figure 1 shows inelastic, exchange, and depletion QM probabilities $P^{J+}_{jK}(E_{col})$ at $J = 0$ and 15, $p = +$, $j = 2$ and 4, and $K = 0$ and 2. The reactions do not have thresholds because the $\tilde{A}^2A'$ PES is barrierless and NH is vibrationally excited. As was observed for NH($a$,0) + H′,[15] the probabilities display many strong and sharp resonances because of the deep potential well, mainly for the inelastic collision at low $E_{col}$ and $J = 0$. The insertion mechanism and the long-lived collision complexes found[9,15] at $v = 0$ thus persist at $v = 1$. However, these resonances are reduced at high $J$ by the averaging effect of the Coriolis couplings.

The inelastic probabilities for NH($a$,1) + H′ → NH($a$,0) + H′ are larger than the reactive ones by a factor of two or three. Therefore, intramolecular energy transfer within the collision complexes is preferred to the breaking and formation of chemical bonds.

We also see that high $J$ and $K$ values enhance the probabilities of the inelastic products NH($a$,0) + H′ and of the exchange ones NH′($a$,0) + H, whereas they lower the depletion channel to N($^2D$) + $H_2$. The projections of the overall WP on the Ω states strengthen this scenario, showing that inelastic and exchange probabilities are enhanced by large Ω values as well. These Ω effects are similar to those found for NH($a$,0) + H′.[15] They are associated with negative centrifugal and Coriolis terms at high $J$ and Ω and with the reaction stereodynamics at large Ω that favor a nearly straight attack of H′ on N, thus giving preferentially inelastic or exchange products.

Finally, initial rotation, $j$, of NH($a$,1) inhibits inelastic collisions but has little effect on the reactive processes.

## 6. Cross Sections

We plot in Figure 2 BO QM, and QCT cross sections $\sigma_j(E_{col})$ for inelastic, exchange, and depletion collisions. QM and QCT results agree remarkably well, although quasiclassical calculations cannot reproduce the quantum-mechanical resonances. The inelastic QCT cross sections are too high at very small collision energies and slightly too low at high $E_{col}$, the exchange ones are always slightly low, and the depletion ones show the best agreement.

At low $E_{col}$, the QM cross sections display distinct resonances up to ∼0.06 eV. We find QM thresholds at ∼0.007 eV and sharp increases up to ∼0.015 eV and ∼21 Å$^2$ for the inelastic channel, followed by an average decrease at higher energies due to the barrierless nature of the PES. The inelastic cross section is by far the largest at all collision energies. Reactant rotational excitation slightly inhibits the low-energy reactivity, owing to the associated centrifugal barrier, but it does not significantly affect the cross sections at larger $E_{col}$.

Compared with NH($v = 0$) + H′ reactions,[15] the present $v = 1$ exchange cross sections are slightly larger at low collision energy but become smaller by more than a factor of two at high energies. On the other hand, NH vibrational excitation inhibits the depletion reaction by ∼24 and 37% at low and high $E_{col}$, respectively. This implies that the vibrational relaxation of NH($v = 1$) to NH($v = 0$), induced by the collisions with H′, occurs at the expense of the reactive processes.

We have also calculated QM and QCT cross sections for the formation of NH($v' = 1$) or NH′($v' = 1$), that is, elastic breakup of the complex without vibrational relaxation to $v' = 0$, although they are not observable in the experiment. In brief, QM and QCT results agree and increase with $E_{col}$ from a small fraction to about 50% of the total cross section.

## 7. Rate Constants

Table 3 presents BO inelastic, exchange, and depletion initial-state-resolved rate constants $k_j(300)$ and thermal rates $k(T)$, at $T = 300$ K, including the 1/2 electronic degeneracy factor. We compare QM and QCT results, and we also report the total experimental loss rate $k_{loss}$ at room temperature.

(1) QM rates. As expected from the probabilities and cross sections, the inelastic collisions make the largest contribution to $k_{loss}$. In fact, the inelastic rate is equal to 69% of the total loss rate, and this factor does not depend on $j$. Of the two reactions, exchange is favored by a constant factor of ∼1.7; that is, exchange and depletion reactions contribute to the total reactivity by ∼19.5 and 11.5%, respectively. All QM rates are slightly inhibited by NH rotational excitation, and thus $k_5/k_2 \approx 0.75$. We also report QM exchange and depletion rates for NH($v = 0$) + H′ reactions,[15] showing that competition from the inelastic channel reduces both of those rates.

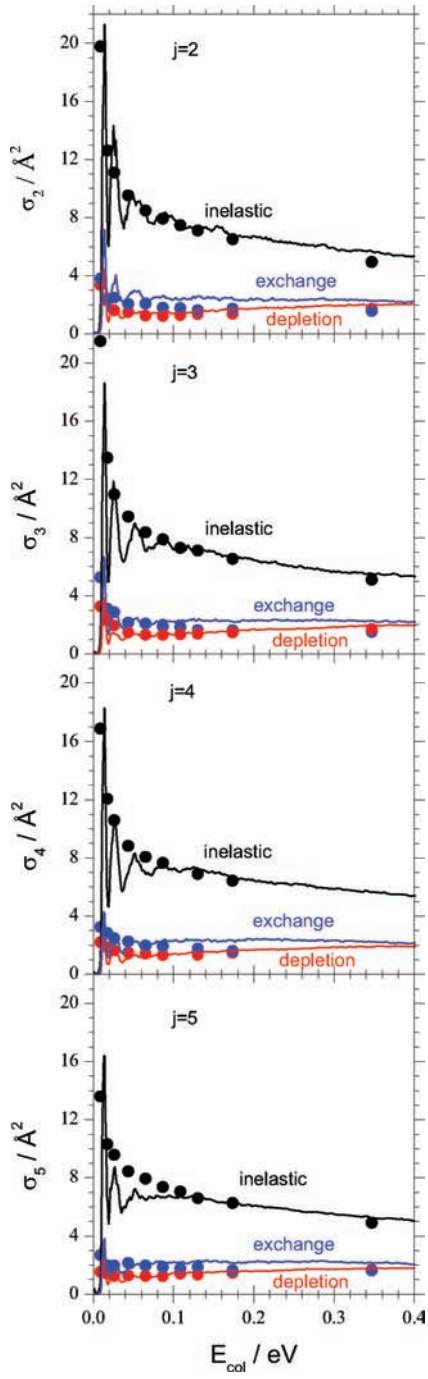


**Figure 2.** BO QM (—), and QCT (●) cross sections $\sigma_j$, for inelastic to NH($a$,0) + H′, exchange to NH′($a$,0) + H, and depletion to N($^2D$) + $H_2$. $j$ = 2, 3, 4, and 5.

(2) QCT rates. These are generally larger than the QM rates, save for the $j = 2$ exchange coefficient, $k_2$. The overestimation of the rates is due to the overestimation of the near-threshold cross sections by the classical calculations. For $j = 2$, QM and QCT total rates agree quite well, owing to a compensation of errors for the results of the various collisions. The agreement is less good when NH is rotationally excited, mainly at $j = 3$, where QCT inelastic and depletion rates $k_3$ are larger by 25 and 28%, respectively. Therefore, QCT rates do not decrease monotonically with $j$ but have a maximum at $j = 3$.

(3) Theoretical and experimental total loss rates $k_{loss}$. Table 3 shows that QM, QCT, and experimental $k$(300) are equal to 13.8, 15.6 ± 1.6, and (9.1 ± 3.3) × $10^{-11}$ $cm^3$ $s^{-1}$, respectively. The QM value increases to 14.4 ± 0.5 if we estimate the $j$ = 6 contribution via an extrapolation of those calculated at lower $j$. The QM error bars take into account this extrapolation and the interpolation approximation of some probabilities. The QCT value includes $j$ values up to 6 and is only 8% larger than the QM value. The theoretical loss rate coefficients thus agree well. However, they are substantially larger than the experimental value and are outside its estimated limits of error. Some systematic error therefore remains in the calculations, the experiment, or both.

The possible sources of error in the calculations include the PES, the dynamics calculations (including the possibility of nonadiabatic effects), and the averaging. Our purpose in carrying out QM and QCT calculations independently was to test the possibility of significant error in the dynamics calculations. The good agreement between those two sets of results and the clear explanations for the disagreements that remain indicate that the classical model is reasonable and that both the QCT and WP BO calculations are adequately converged. The averaging procedure is also probably adequate; the collision energies and initial states used in the QM and the QCT treatments were different, but the two treatments gave consistent results. Remaining possible sources of theoretical error are the potential surfaces themselves and the simple treatment of nonadiabatic effects. Evidence of neglect of RT coupling being acceptable has already been presented, so we now examine the quality of the PES.

The dynamics are dominated by the complex formation step, which is sensitive to the long-range part of the PES. It is certainly possible that errors in the long-range attraction might cause an overestimation of the complex formation rate and therefore of the total loss rate. We checked this possibility by performing electronic structure calculations in the NH($a^1\Delta$) + H channel, as described in ref 8, but for different atomic basis sets: aug-cc-pvtz, aug-cc-pvqz, and aug-cc-pv5z.[24] The potential energies for the aug-cc-pvqz and aug-cc-pv5z basis sets essentially agree, and the energies for the much smaller aug-cc-pvtz basis set are only marginally higher. The PESs used in the dynamics study were calculated with the aug-cc-pvqz basis set. We conclude that the PES is probably not the cause of the overestimation of the loss rate.

Errors in the experiment are also possible. However, most systematic errors would tend to increase the observed loss rate rather than decrease it, and correction for those errors would not improve the agreement with theory. An unaccounted source that replenishes NH($a$,1) could lower the rate coefficients, but in most cases would lead to clearly nonexponential loss profiles. Those were not observed, and we regard the stated error bounds as being realistic.

BO thermal rates from the QM and QCT calculations are plotted in Figure 3 together with the room-temperature measured rate $k_{loss}$. The theoretical values include $j$ levels up to 8 at 500 K, calculated explicitly or estimated from fits. We fitted the QM rate constants to the standard Arrhenius expressions $k(T) = A \exp(-E_a/k_BT)$, finding the parameters listed in Table 4. Owing to this fitting approximation, the QM error bars of $k$(500) and $A$ are equal to ±10 and ±7%, respectively. All reactions have small activation energies, as expected because the PES is barrierless and the centrifugal barriers are small. The rates thus increase modestly with $T$.

## 8. Summary

We have presented a calculation of a room-temperature rate coefficient for a reaction involving an electronically excited reactant and a long-lived complex from first principles. By

**TABLE 3: NH($a$,1) + H′[a]**

| | inelastic to NH($a$,0) + H′ | | exchange to NH′($a$,0) + H | | depletion to N($^2D$) + $H_2$ | | total | |
|---|---|---|---|---|---|---|---|---|
| $j$ | QM | QCT | QM | QCT | QM | QCT | QM | QCT |
| 2 | 11.6 | 12.6 | 3.49 | 2.77 | 1.95 | 2.03 | 17.0 | 17.4 |
| 3 | 10.2 | 12.8 | 2.94 | 3.07 | 1.67 | 2.14 | 14.8 | 18.0 |
| 4 | 9.65 | 11.8 | 2.61 | 2.84 | 1.56 | 1.93 | 13.8 | 16.6 |
| 5 | 8.85 | 11.0 | 2.41 | 2.54 | 1.47 | 1.66 | 12.7 | 15.2 |
| thermal | 9.50 | 11.2 | 2.73 (3.02)[b] | 2.61 | 1.57 (2.77)[b] | 1.81 | 13.8 (14.4 ± 0.5)[c] | 15.6 ± 1.6 |
| experiment | | | | | | | 9.1 ± 3.3 | |

[a] BO initial-state-resolved rate constants $k_j$ and thermal rate constants $k$ at $T = 300$ K, in $10^{-11}$ cm$^3$ s$^{-1}$, including the 1/2 electronic degeneracy factor. [b] NH($a$,0) + H′, from ref 15. [c] Including a $k_6$ estimate.

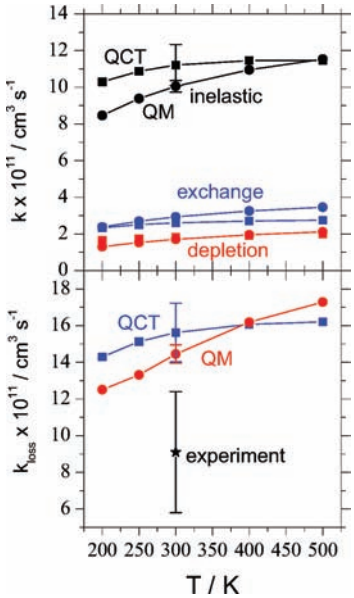


**Figure 3.** Above: BO QM (●), and QCT (■) thermal rate constants for inelastic, exchange, and depletion channels. Below: theoretical BO and experimental total loss rate constants. The 1/2 electronic degeneracy factor is included in the calculated values.

**TABLE 4: NH($a$,1) + H′[a]**

| | $A \times 10^{11}$/cm$^3$ s$^{-1}$ | $E_a$/eV |
|---|---|---|
| inelastic to NH($a$,0) + H′ | 14.2 | 0.009 |
| exchange to NH′($a$,0) + H | 4.44 | 0.011 |
| depletion to N($^2D$) + $H_2$ | 2.91 | 0.014 |
| total loss | 21.5 | 0.010 |

[a] BO QM Arrhenius parameters.

means of QM WPs and quasiclassical trajectories, we studied the dynamical processes occurring in collisions of vibrationally and electronically excited NH($a^1\Delta$, $v = 1$) with H($^2S$): vibrational relaxation to NH($a^1\Delta$, $v = 0$), H atom exchange, and depletion to N($^2D$) + $H_2$. Most of the calculations were performed using only the PES of the $\tilde{A}^2A'$ excited state of $NH_2$, that is, nonadiabatic Renner−Teller-induced transitions to the $\tilde{X}^2A''$ ground state were neglected. In the QM calculations, Coriolis couplings were fully taken into account, and in the QCT study, only trajectories that ended with vibrational energy close to a quantum vibrational level of the diatom were processed.

The initial-state-resolved QCT cross sections for relaxation, exchange, and depletion agree well with the corresponding QM cross sections over a large range of collision energies. Pronounced resonance structures at very low energies, due to the deep potential well, are not reproduced by the trajectory calculations. The resulting thermal rate coefficients between 200 and 500 K slightly increase with temperature, as is typical for an attractive potential without a barrier. Pure vibrational relaxation contributes about 69% of the total computed loss, relaxation with exchange contributes about 20%, and depletion contributes the remaining 11%.

The theoretical studies are accompanied by an experimental measurement of the room-temperature rate coefficient for the total loss of NH($a$,1) in collisions with H. The measured rate coefficient includes loss from vibrational relaxation with and without H atom exchange, depletion to N($^2$D) + $H_2$, and electronic quenching to NH($X^3\Sigma^-$) induced by RT transitions. The QM and QCT rate constants for the loss of NH($a$,1) agree within their estimated error margins. However, they overestimate the experimental rate by about 60%, an amount outside the experimental error limit.

The cause of the disagreement is not clear. The quality of the PES has been tested by the earlier work on NH($a$,0) + H[9,15] and by a separate basis set convergence check presented here. Our TSH calculations indicated that RT effects on the total loss rate were negligible, so neglecting these couplings cannot be the cause of the disagreement unless the empirical model of Adam et al.[9] is very badly in error. In any case, including RT effects in the calculations would worsen the disagreement rather than mitigate it. The accuracy of the single-surface dynamics calculations is supported by the good agreement between our independent QM and QCT calculations. It is most likely that some combination of small errors in the potential, dynamics, and experiment is causing our substantial disagreement.

**Acknowledgment.** This work was supported by MIUR and IPCF-CNR of Pisa and by the Max-Planck-Institut für Dynamik und Selbstorganisation.

**Note Added after ASAP Publication.** This Article was published on Articles ASAP on July 1, 2009. Footnote *d* of Table 1 was changed to "1000/s" and the citation for ref 1 after "PESs" in line 5 of section 4 was removed. The corrected version was posted on July 27, 2009.

## References and Notes

(1) Jungen, C.; Hallin, K.-E. J.; Merer, A. J. *Mol. Phys.* **1980**, *40*, 25.
(2) Dixon, R. N.; Irving, S. J.; Nightingale, J. R.; Vervloet, M. *J. Chem. Soc., Faraday Trans.* **1991**, *87*, 2121.
(3) Gabriel, W.; Chambaud, G.; Rosmus, P.; Carter, S.; Handy, N. C. *Mol. Phys.* **1994**, *81*, 1445.
(4) Koshi, M.; Yoshimura, M.; Fukuda, K.; Matsui, H.; Saito, K.; Watanabe, M.; Imamura, A.; Chen, C. *J. Chem. Phys.* **1990**, *93*, 8703.
(5) Davidson, D. F.; Hanson, R. K. *Int. J. Chem. Kinet.* **1990**, *22*, 843.
(6) Suzuki, T.; Shihira, Y.; Sato, T.; Umemoto, H.; Tsunashima, S. *J. Chem. Soc., Faraday Trans.* **1993**, *89*, 995.
(7) Adam, L.; Hack, W.; Zhu, H.; Qu, Z.-W.; Schinke, R. *J. Chem. Phys.* **2005**, *122*, 114301.

(8) Qu, Z.-W.; Zhu, H.; Schinke, R.; Adam, L.; Hack, W. *J. Chem. Phys.* **2005**, *122*, 204313.
(9) Adam, L.; Hack, W.; McBane, G. C.; Zhu, H.; Qu, Z.-W.; Schinke, R. *J. Chem. Phys.* **2007**, *126*, 034304.
(10) Pederson, L. A.; Schatz, G. C.; Ho, T.-S.; Hollebeek, T.; Rabitz, H.; Harding, L. B.; Lendvay, G. *J. Chem. Phys.* **1999**, *110*, 9091.
(11) Pederson, L. A.; Schatz, G. C.; Hollebeek, T.; Ho, T.-S.; Rabitz, H.; Harding, L. B. *J. Phys. Chem. A* **2000**, *104*, 2301.
(12) Ho, T.-S.; Rabitz, H.; Aoiz, F. J.; Bañares, L.; Vázquez, S. A.; Harding, L. B. *J. Chem. Phys.* **2003**, *119*, 3063.
(13) Poveda, L. A.; Varandas, A. J. C. *Phys. Chem. Chem. Phys.* **2005**, *7*, 2867.
(14) Gamallo, P.; Defazio, P.; González, M.; Petrongolo, C. *J. Chem. Phys.* **2008**, *129*, 244307, and references therein.
(15) Akpinar, S.; Defazio, P.; Gamallo, P.; Petrongolo, C. *J. Chem. Phys.* **2008**, *129*, 174307.
(16) Hack, W.; Wilms, A. *J. Phys. Chem.* **1989**, *93*, 3540.
(17) Hack, W.; Mill, T. *J. Phys. Chem.* **1993**, *97*, 5599.
(18) Tezaki, A.; Okada, S.; Matsui, H. *J. Chem. Phys.* **1993**, *98*, 3876.
(19) Gray, S. K.; Balint Kurti, G. G. *J. Chem. Phys.* **1998**, *108*, 950.
(20) Meijer, A. J. H. M.; Goldfield, E. M.; Gray, S. K.; Balint Kurti, G. G. *Chem. Phys. Lett.* **1998**, *293*, 270.
(21) Truhlar, D. G.; Muckerman, J. T. In *Atom-Molecule Collision Theory: A Guide for the Experimentalist*; Bernstein, R., Ed.; Plenum: New York, 1979; p 505.
(22) Varandas, A. J. C. *J. Chem. Phys.* **1993**, *99*, 1076.
(23) Fleurat-Lessard, P.; Grebenshchikov, S. Y.; Schinke, R.; Janssen, C.; Krankowsky, D. *J. Chem. Phys.* **2003**, *119*, 4700.
(24) Dunning, T. H., Jr. *J. Chem. Phys.* **1989**, *90*, 1007.

JP903839P